

Abstract

14

15

16 Patterns and trends of sea level rise in the regional seas around Taiwan are
17 investigated through the analyses of long-term tide-gauge and satellite altimetry data.
18 The 50 year-long time series reveal decadal and interannual variations and
19 spatially-inhomogeneous patterns of generally rising sea level. The East Asia
20 tide-gauge stations around Taiwan show an average trend of +2.4 mm/yr from
21 1961-2003 which is larger than the reported global rate of +1.8 mm/yr for the same
22 period. These stations also show significantly larger sea level rise rates (5.7 mm/yr)
23 than global values (3.1 mm/yr) during the period from 1993-2003. Consistent with the
24 coastal tide-gauge records, satellite altimetry data show similar increasing rates (5.3
25 mm/yr) around Taiwan during the same period. The slightly higher values from the
26 tide gauges could be due to local subsidence. Further comparisons with temperature
27 anomalies in the upper ocean suggest that thermal expansion and heat advection in the
28 upper layer contribute significantly to the long term sea level variations in this area
29 with correlations > 0.9 for observations after 1992. The thermosteric sea-level
30 variations may explain the interannual and decadal variations of the observed sea
31 level rises around Taiwan. Our analysis also indicates that the altimetry data is only a
32 part of a long-term and larger-scale signal. Finally, we find that a non-linear smoother,
33 namely LOESS, is more suitable for extracting long-term trends in sea level than the
34 traditional linear regression approach.

35

36 **1. Introduction**

37

38 Estimates of twentieth century Sea Level Rise (SLR) are primarily based on coastal
39 tide gauges, which measure the sea surface height relative to coastal benchmarks and
40 often provide long and unique time series. In general, global SLR results from two
41 mechanisms: (1) steric effects: volume change due to seawater density change in
42 response to temperature (thermosteric) and salinity (halosteric) variations; and (2)
43 eustatic effects: mass change due to exchange of water with the atmosphere and
44 continents, such as from glaciers and ice sheets, through precipitation, evaporation,
45 river runoff, and ice melting. However, neither of these processes is currently well
46 understood.

47

48 Although coastal tide gauges provide the longest records for estimating SLR, these
49 measurements may include other signals such as local subsidence, tectonic motion,
50 and secular trends in vertical movement of the earth's crust and sea surface, e.g.,
51 Glacial Isostatic Adjustment (GIA). The GIA is due to the transfer of mass from the
52 ice sheets to the oceans, thus alleviating the loading of the earth, and small
53 spatial-scale tectonic motions ([Intergovernmental Panel on Climate Change, IPCC,](#)
54 [2007](#)). It can be roughly corrected using geophysical models (e.g., Tushingham and
55 Peltier, 1991), while the local tectonic and subsidence motions are not easily detected
56 and estimated. Douglas (1997) estimated a globally averaged SLR rate of 1.8 mm/yr
57 using 24 long tide-gauge records after applying GIA corrections. Miller and Douglas
58 (2004) further showed that twentieth century SLR was +1.5~2.0 mm/yr, which
59 includes both volume (steric) and mass (eustatic) changes. This is approximately 2~3
60 times higher than the rates (0.5 mm/yr) due to volume changes derived from
61 temperature and salinity data only. Satellite-based estimates suggest that SLR has

62 increased at an even faster rate of 2.8 ± 0.4 mm/yr since the 1990s (IPCC, 2007).
63
64 Furthermore, some studies suggest that regional differences in SLR may contribute to
65 large spatial variations in the rate of global SLR (e.g., Church et al., 2004). Larger
66 SLR has been identified in the western tropical Pacific, eastern Indian, and Southern
67 oceans during the last decade (Cazenave et al., 2002; Li et al., 2002). These studies
68 showed the importance of regional SLR and understanding its causes. There are few
69 sea level studies of the regional seas around Taiwan, and none has yet focused on the
70 potential impacts of SLR to Taiwan. Chen (1991) reported SLR at the Changjiang
71 river mouth since the early 1920s. Wang (1998) further estimated the rate of SLR of
72 $+2\sim 3$ mm/yr along the coast of China during the last century. Overpumping of
73 groundwater and overloading by construction on the delta plain and lowland coast
74 have had serious effects: the average rate of relative SLR is $+24.5\sim 50$ mm/yr in
75 Tianjing (north China) and $+6.5\sim 11.0$ mm/yr in the Shanghai (SH) area of the
76 Changjiang River (see locations of cities in Figure 1).
77
78 Recently, Li et al. (2002) used TOPEX/Poseidon (T/P) satellite altimetry data to study
79 the general trend in sea level variation in the South China Sea (SCS) between 1993
80 and 2000. They found a rise rate of $\sim +10$ mm/yr with the highest rate of $+27$ mm/yr
81 near the west of Luzon and generally lower rates over the shallow continental shelves.
82 They attributed the rapid rise in sea level to the rapid warming of the upper layer in
83 the SCS. Cheng and Qi (2007) further analyzed longer satellite altimetry data series
84 (October, 1992~January 2006) in the SCS. They found a rise rate of 11.3 mm/yr
85 during 1993~2000 and, subsequently, a negative rate of -11.8 mm/yr during
86 2001~2005. The asymmetric distribution of sea level variations over the SCS suggests
87 pronounced variations in this area and the influence of thermal advection.

88

89 Levitus et al. (2000) showed that the world's oceans have been warming over the last
90 50 years, with substantial changes in heat content occurring in the upper 300 m to
91 1000 m in each ocean. Substantial changes in North Atlantic heat content also occur at
92 depths greater than 1000 m. Levitus et al. (2005) further estimated that the global
93 oceanic heat content (OHC) increased by approximately 14.5×10^{22} J during
94 1955~1998. The global mean temperature also increased by 0.037 °C for the whole
95 ocean (0–3000 m) and 0.171 °C for the upper layer (0–300 m). Thermal expansion
96 associated with this warming of the ocean should be associated with a corresponding
97 SLR. Cabanes et al. (2001) reported that the global mean SLR over 1993~2000
98 reached 3.2 ± 0.2 mm/yr, close to the estimated 3.1 ± 0.4 mm/yr based on
99 thermosteric SLR integrated down to 500 m. They also showed that the thermosteric
100 SLR was 0.5 ± 0.05 mm/yr during 1955~1996. Using the salinity data for 1957~1994,
101 Antonov et al. (2002) suggested that the input of fresh water to the oceans could
102 explain the remaining SLR. A decrease in global mean salinity during 1957~1994 and
103 this equivalent increase in fresh water could cause global sea level to increase at a rate
104 of 1.3 ± 0.5 mm/yr if the added water came from sources other than floating sea ice.
105 Also, spatially-inhomogeneous patterns exist based on their data (Antonov et al.,
106 2002).

107

108 Taiwan is an isolated island located at the western edge of the Pacific, at the point
109 where the East China Sea (ECS), the Philippine Sea (PS), and the SCS join. An active
110 tectonic oblique convergence exists around Taiwan so that the island is considered to
111 have been tectonically active for the past two million years (Ho, 1986). The
112 surrounding bathymetry is complicated (Figure 1). West of the Taiwan island is the
113 Taiwan Strait, a 200-km-wide shallow passage (less than 100 m in general) between

114 Taiwan and mainland China. The Taiwan Strait is part of the regional sea off eastern
115 China. It forms a topographic barrier inhibiting the intermediate- and deep-water
116 circulation. East of Taiwan, the bathymetry drops rapidly down to 4000 m from the
117 coastline. Such steep relief is truncated by the Ryukyu Trench and the Okinawa
118 Trough to the north, which correspond to the northward subduction of the Philippine
119 Sea basin beneath the southeast Chinese continental margin (Figure 1). South of the
120 island of Taiwan is the Luzon-Philippine Archipelago, which is the product of the
121 SCS subduction eastward beneath the Philippine Sea basin. A recent study shows the
122 seamount topography along the northern Luzon-Philippine Archipelago that
123 constrains the Kuroshio to remain primarily in the Pacific Ocean and thus does not
124 intrude far into the SCS (Metzger and Hurlburt, 2001).

125

126 The main objective of this study is to reconstruct the long-term trends of sea level
127 variation in the regional seas around Taiwan and investigate the possible causes of
128 regional SLR. The critical questions we try to answer are: (1) What are the rates of
129 SLR and their long-term variation in the regional seas near Taiwan? (2) How do these
130 rates of SLR compare with those at other locations around the world? (3) What are the
131 possible causes of the SLR in this area? To our knowledge, long-term sea level
132 variations in the regional seas around Taiwan have not been examined and discussed
133 in the literature except for the SCS. Also, the physical processes affecting sea level
134 variations are not well understood. In this study, more than 50 years of tide-gauge data
135 are used to investigate the long-term variations in sea level in the vicinity of Taiwan.
136 Fifteen years of recent satellite altimetry data are also used for comparison and
137 validation. Further details about the impacts of local tectonic changes will be
138 addressed in a separate paper (Chang et al., 2009).

139

140 This paper is organized as follows. In Section 2, the data sources and methods are
141 introduced briefly. Section 3 presents the long-term tide-gauge and satellite altimetry
142 results. Section 4 discusses some possible mechanisms responsible for the SLR.
143 Finally, the conclusions are given in Section 5.

144

145

146 **2. Data sources and methods**

147

148 The data used for our analyses consist of more than 50 years' tide-gauge data
149 (1947~2007 for the longest series) and 15 years of altimetry data. Additional
150 subsurface time series temperature data (Ishii et al., 2006) are also used for
151 comparison. Both tide-gauge and altimetry data are described in this section.

152

153 We have not attempted to apply corrections for GIA or for the inverted barometer
154 effect due to sea level pressure (SLP) in this study. To our knowledge, GIA
155 corrections have yet to be calculated for the study area due to its low latitude (around
156 23.5°N). Also, the expected time scales associated with GIA adjustments are far
157 longer than the time scales of variability in sea level that we consider, and the
158 magnitudes of these corrections are often far smaller than the magnitudes of the sea
159 level variability that we have observed. We have not applied corrections for SLP
160 because, in many cases, observations of SLP at the tide-gauge locations do not exist,
161 or do not exist for the full duration of the tide-gauge records. According to Chelton
162 and Enfield (1986), efforts to separate the local inverted barometer response from
163 other sources of sea level variability have largely been unsuccessful. Finally, it is
164 doubtful that such a correction, if it were applied, would significantly affect any of
165 our conclusions because the magnitudes of variability encountered were relatively

166 large, making it easier to identify the most of the likely sources of variability.

167

168 **2.1 The tide-gauge dataset**

169

170 Figure 1 shows the tide-gauge stations used in this study. The data come from two
171 major data sources: the Central Weather Bureau (CWB), Taiwan, and the Permanent
172 Service for Mean Sea Level (PSMSL²) in Liverpool, England (Woodworth and Player,
173 2003). Information related to each station is also given in Table 1, including
174 information on any movement of the stations. For data sources from CWB, apparent
175 location changes appear for some stations due to changes of management, actual
176 movement of stations, and changes of baselines (see Table 1). All datums are screened
177 carefully for possible artificial datum shifting. For the Taiwan area, we selected three
178 representative stations (Figure 1) from the CWB tide-gauge database. Keelung has the
179 longest time series (dating back to 1946) and is located in north Taiwan. Kaohsiung is
180 located near south Taiwan. Penghu is unique because it is a small island between
181 Taiwan and mainland China in the middle of Taiwan Strait (Figure 1). Tectonically,
182 Penghu is linked to the mainland continent. All of these stations have long, continuous
183 records. **Other CWB stations such as Taichung and Wunkang also have long time**
184 **series but the existence of major gaps limits their overall usefulness in long-term**
185 **evaluations, and thus they have been excluded from this study.**

186

187 All other monthly observations of mean sea level used here have been obtained from
188 the PSMSL (Woodworth and Player, 2003), which covers 287 tide-gauge stations
189 around the world that are part of the Global Sea Level Observing System (GLOSS)
190 monitoring oceanographic sea level and climate change. Note that both Kaohsiung

² <http://www.pol.ac.uk/psmsl/>

191 and Keelung are also available from the PSMSL database but with a few incomplete
192 records. Therefore, we have used the complete records from the CWB database in
193 these areas. The sea level data used in this study are monthly mean values. Note that
194 the “Revised Local Reference” (RLR) data are used here, which are supported by
195 documentation relating measured sea level at each station to a constant local datum
196 over the complete record.

197

198 Since our study emphasizes the long term trend in SLR in the vicinity of Taiwan, the
199 low frequency tidal components such as the nodal tide, which has a period of 18.61
200 years, may affect the record. However, early studies indicated that the amplitude of
201 nodal tide is latitude dependent and has its maxima near the equator and the poles
202 (Lisitzin, 1974). The amplitude is almost negligible near 30–40°N. These features are
203 also typical of the other long-period tidal constituents. Indeed, the comparison with
204 the removal of harmonic nodal mode shows that the influence of long-term nodal tide
205 on our records is minimal near this latitude (not shown here).

206

207 The longest record we employ (Kaohsiung) begins in May 1947 and ends in
208 December 2007, spanning a period of 60 years. Less than 0.5% of the data are missing
209 from each record and so we have used interpolation to complete the time series in
210 each case. It is well known that the island of Taiwan is tectonically active and that
211 there is a major fault line that constitutes a convergent boundary east of Taiwan (light
212 yellow lines on Figure 1). Therefore, we do not consider the tide-gauge stations along
213 the east coast, where greater vertical motion is expected. The measurement sites
214 chosen for this study are located on the same tectonic plate and any vertical
215 displacement due to the plate motion assumes to be small. Tectonic influences will be
216 discussed further in a separate paper.

217 **2.2 Satellite altimetry**

218

219 Since the tide-gauge measurements include many other contributions, such as tectonic
220 movements and local subsidence, and observations are limited to coastal regions,
221 satellite altimetry provides an alternative to detect regional sea level variations with
222 more comprehensive spatial coverage. **To estimate relative SLR in recent years, we**
223 **also use 15 years' altimetry data of the Radar Altimeter Database System (RADS)**
224 **from 1993 to 2007 (Schrama et al., 2000).** The RADS altimetry data are used here for
225 comparison and validation. The RADS provides a well validated and cross-calibrated
226 sea level dataset, including European Remote Sensing (ERS), T/P, and Geosat data. It
227 operates within the framework of the Netherlands Earth Observation NETwork,
228 NEONET, an Internet facility funded by the Dutch government. Figure 2 shows the
229 altimetry tracks used in this study, where we have divided the seas around Taiwan into
230 five regions (A–E).

231

232 **3. Results**

233

234 **3.1 Estimating long-term (decadal) trends from the tide-gauge records**

235

236 First, we show the sea levels observed at several different stations and plotted in
237 millimeters (mm) as a function of time. Monthly mean sea levels and their trends over
238 a period of more than 50 years are shown in Figures 3 and 4. These panels are ordered
239 based on the individual station's relative tectonic plate location and latitude. Figure
240 3(a) shows the monthly observations of relative sea level in Hong Kong and
241 Kaohsiung for the period from 1950 through 2007. Both locations reflect similar
242 coastal responses around the SCS. In order to remove the seasonal, annual, or other

243 high frequency signals, an 18-month moving mean filter (shown as dashed lines) has
244 been applied to the scattered observations (shown as dots). The moving mean filter is
245 commonly used to estimate the SLR and is well known to distort the content of the
246 signal in the frequency domain (e.g., Emery and Thomson, 2004). Its major problem
247 is its inability to identify non-linear variations such as the length or duration of the
248 trends. In order to capture non-linear trends in sea level, a locally weighted running
249 line smoother called LOESS (Cleveland, 1979; Hastie and Tibshirani, 1990;
250 Cleveland and Devlin, 1988) is applied and compared with the robust linear
251 regression trend. **It is often used to estimate non-linear trends where non-linearity is**
252 **important.** Note that two nearby observations are shown for Hong Kong, obtained
253 from the records at PSMSL. These nearby stations (HK and TP) show similar
254 long-term trends except for possible phase differences and local deviations, as
255 expected. The existence of local variations is not surprising and emphasizes the
256 spatial inhomogeneity of sea level variations. The long-term increase in sea level is
257 clear between 1950 and the 2000s, and some major decadal oscillations can also be
258 observed (e.g., in the 1950s, late 1970s, and late 1990s). Although we recognize the
259 likely influence of tectonic effects, the time scales associated with tectonic subsidence
260 and uplift are expected to be much longer than the timescales we refer to here.

261

262 Figure 3(b) shows the mean sea level variations at Xiamen and Penghu. Both tide
263 gauges show similar peaks during the 1970s. The sudden decrease in slope around
264 1980 is striking. To verify this tendency, and to compare the actual rates of change in
265 sea level together, we have calculated and compared the yearly forward first
266 differences, which represent the yearly slopes (Figure 5). The average of all slopes
267 during a particular period represents the long-term mean slope (linear trend) for that
268 period. We find that this approach is better and easier to apply than fitting a straight

269 line to the entire record because a straight linear regression completely ignores the
270 possibility that the long-term slope may be non-linear, as shown here.

271

272 Figure 4 shows the remaining observations north of Taiwan. All stations exhibit
273 similar trends except Keelung. The large increase in sea level during the late 1970s is
274 much weaker and limited at Keelung. It is also reported that extraordinary subsidence
275 at the Keelung station occurred at least in the early 90s (Chang et al., 2009).

276 Nevertheless, the 18-month moving mean for Keelung detects weaker but still
277 increasing trends for the same period, which are generally consistent with those
278 detected by the other stations. Figure 5 clearly shows the rates of change for each year.
279 The rates of increase drop rapidly after 1980 and even become negative, upon
280 occasion, by the late 1990s. We note that during the period between about 1960 and
281 2000, although the rates of change vary, there is some degree of constancy. In general,
282 these tide-gauge data show similar trends and decadal variations with different
283 maxima occurring locally with phase differences (e.g., late 1950s~early 1960s:
284 decreasing; 1970s: increasing; 1980s: increasing weakly; late 1990s: increasing), but
285 yet suggest that regional sea level is varying in a coherent manner at low frequencies.
286 These characteristics are summarized below.

287

- 288 1. Long-term increases in SLR since 1950 are observed consistently at all stations
289 regardless of the analysis technique employed. Similar trends are frequently
290 observed except for local differences (e.g., Keelung shows a very smooth
291 long-term trend while variations can still be detected from the moving mean).
- 292
- 293 2. The non-linear trends of sea level in the regional seas around Taiwan contain a
294 significant amount of interannual and decadal variability, the existence of which is

295 coherent in all records with remarkable falls and rises occurring in a cyclic manner.
296 All stations show SLR maxima during the 1970s and 1990s. The signals at Penghu
297 and Keelung are weaker due to possible local vertical motions of the measurement
298 platform.

299

300 3. The most recent significant increase of SLR in the regional seas around Taiwan
301 occurred in the late 1990s. Consistent with global and other regional observations,
302 all sea level curves show a rise of more than 10 mm/yr followed by a sea level fall
303 accompanying the 1997~1998 ENSO (Figure 5).

304

305 4. In general, the current long-term reconstruction of sea level shows clear
306 indications of decadal oscillations. From these long records, the most recent 15
307 years' variation (1993~2007) may correspond to initially increasing and then
308 decreasing phases (after 2000) of the decadal oscillation in sea level. Significant
309 interannual and multi-year variability indicates the need for long records to
310 reliably estimate the long-term rate of SLR from individual sites, which is
311 consistent with previous recommendations (e.g., Douglas, 1997).

312

313 **3.2 General SLR features from the tidal-gauge and altimetry data over the last** 314 **15 years**

315

316 Satellite altimetry has only been available since the early 1990s. The
317 altimetry-derived rates of sea level variation during the period 1993~2007 in the
318 regional seas around Taiwan are presented in Figure 6. Five locations are shown
319 around Taiwan and the spatial inhomogeneity is clear. Even though altimetry data
320 show a generally increasing trend at all locations, there is considerable spatial

321 variability. Based on the forward first differences from LOESS smoothing of the
322 altimetry data, the mean trend of SLR is +5.0 mm/yr between 1993 and 2007 around
323 Taiwan (Table 2). Linear regression analysis gives a lower rate of +3.7 mm/yr (labeled
324 on panels). This lower rate is not surprising because the non-linear variation (first
325 increasing and then decreasing after 2000) cannot be fully captured by linear
326 regression.

327

328 All observations show SLR of at least 4~5 mm/yr except at location E (the linear
329 regression trend is only 0.92 mm/yr), where some satellite observational uncertainties
330 may exist due to the shallowness of the Taiwan Strait (the maximum depth is 60–70
331 m). Panels B and C, both located east of Taiwan, show quite similar variations (**trends
332 and phases, correlation $r = 0.95$**). The sea level variations at E are close to the
333 northeast corner of the SCS and so they should be associated with the regional
334 response in the SCS. The spatial inhomogeneity of sea level trends around Taiwan is
335 not well understood but may be linked to the regional ocean dynamic and
336 thermodynamic processes. Previous studies also suggest that the sea surface
337 temperature anomaly (SSTA) in the SCS is correlated with the eastern Pacific SSTA at
338 a half-year lag (Ose et al., 1997; Xie et al., 2003). Large rates of sea level variation
339 tend to occur east of Taiwan (e.g., in Zones B and C) with a relative maximum SLR
340 around early 1998 (some delayed variations are also observed at other stations), which
341 may be associated with the 1997~1998 El Niño. The relative maximum in the late
342 1990s is consistent with the tide-gauge data in Figures 3 and 4, indicating the
343 extensive nature of the SLR signals. This appears to result from the long-term
344 variations in the upper OHC down to a depth of a few hundred meters. The variation
345 in the temperature anomaly above the 14 °C isotherm in the Pacific Ocean (Palmer et

346 al., 2007)³ is also presented in Figure 6(a) based on an 18-month moving mean. The
347 correlation, r , with location A is as high as 0.91, with a one-year delay (> 0.79 if no
348 phase shift is considered). For all other stations r is also greater than 0.86. This
349 analysis provides a more consistent view of the underlying warming and its
350 connection with the SLR near Taiwan. When the OHC increases, sea levels at
351 locations B and C rise through thermal expansion as a result of advection from the
352 warm Kuroshio. More discussion about the OHC is presented in Section 4.

353

354 In order to further investigate sea level variations in the most recent 15 years and to
355 verify the coastal tide-gauge data, the altimetry-derived SLRs (location E) are also
356 compared with the sea level variations at the nearest coastal tide gauge (Kaohsiung,
357 KS) for the same time period in Figure 7. The altimetry-derived sea level anomalies
358 are generally coincident with the tide-gauge data, including the minimum around
359 1996 and maximum around 2000. Based on the LOESS, the estimated SLR values
360 from 1993 to 2007 according to the tide-gauge and altimetry (E) are 3.6 mm/yr and
361 3.1 mm/yr, respectively. The difference is small. However, a large difference is found
362 by using linear regression analysis: the trends are 7.54 mm/yr and 4.46 mm/yr,
363 respectively. Our results suggest that linear trends may not always be representative
364 for regional sea level variations. The LOESS analysis is better for estimating
365 non-linear trends than traditional linear regression because it is based on local
366 regression rather than regression applied to the entire record (Breaker, 2007).
367 Regardless of the analysis methods, the tide-gauge determined trend at Kaohsiung is
368 always larger than that estimated from altimetry. Land subsidence around
369 southwestern Taiwan could be a possible contributing factor. Unfortunately, the actual
370 magnitude of this effect is unclear.

³ <http://hadobs.metoffice.com/hadgoa/>

371

372 After 2001, both types of observations show a pronounced fall and the trend of
373 decreasing sea level continues for the next four years, followed by increasing sea level
374 after 2005 (Figure 7). These variations in sea level are an important feature in the SCS
375 (e.g., Cheng and Qi, 2007). We also find that the variations in the tide-gauge
376 determined SLR agree well with the variations in the temperature anomalies in the
377 SCS; see the thick solid line in Figure 7 for the long-term depth integrated (down to
378 300 m) temperature anomaly in the northeastern SCS (Ishii et al., 2006). The
379 temperature anomalies and the sea level variations from the two sources are similar
380 except for slight differences during the 1997~1998 El Niño. The altimetry-derived sea
381 levels show a larger increase while both tide-gauge data and the observed temperature
382 anomaly exhibit similar trends. The agreement between the tide-gauge determined
383 SLR and the temperature anomaly supports the idea that regional ocean warming
384 plays an important role in the observed sea level variations. The correlation is close to
385 0.9 while it is only 0.81 between the altimetry-derived SLR and the temperature
386 anomaly.

387

388 **Our results suggest that over the last 15 years sea levels around Taiwan have risen and**
389 **appear to be associated with thermal expansion. The recent large variations in the**
390 **regional seas around Taiwan could be transient, as suggested by the increasing rates of**
391 **SLR during the late 1990s followed by decreases in the rate of SLR. However,**
392 **comparing the long term variations in the tide-gauge data with the results of the**
393 **15-year period of satellite altimetry may not allow us to infer long-term climate**
394 **changes, due to the apparent lack of decadal influences in the trends.**

395

396 **3.3 Regional variations and the relation between the regional seas around Taiwan**

397 **and the global ocean**

398

399 Table 2 compares the mean sea level trends during several periods since 1955. These
400 are mainly computed from data collected at eight coastal stations in the regional seas
401 around Taiwan. For the recent period of 1993~2003, the tide-gauge determined mean
402 SLR is 5.7 mm/yr (Table 2), slightly higher than that estimated from the altimetry data
403 (5.3 mm/yr). These values are also similar to those estimated in other western Pacific
404 (WP) regions and are much higher than the observed global mean of 3.1 ± 0.7 mm/yr
405 for the same period (IPCC, 2007). For example, Kang et al. (2005) reported average
406 trends of 5.4 mm/yr for the entire East/Japan Sea (EJS), and 6.6 mm/yr for the
407 southern EJS during 1992~2001. Cheng and Qi (2007) found a rise rate of 11.3 mm/yr
408 during 1993~2000 and, subsequently, a decline rate of -11.8 mm/yr during 2001~2005
409 in the SCS. These large rates of change in the regional seas around Taiwan may be an
410 extension of the larger trend in the WP shown in earlier results (Cabanés et al., 2001;
411 Li et al., 2001; Kang et al., 2005) and reflect the regional response to interannual
412 climate variability. In recent decades, the altimetry data also reveal a large-scale
413 pattern of sea level change, with sea level falling in the eastern Pacific and rising in
414 the WP (IPCC, 2007).

415

416 Based on the coastal tide-gauge data from locations near Taiwan, Table 2 also shows
417 mean rates of rise of 3.5 mm/yr from 1955~2003 and 2.4 mm/yr from 1961~2003,
418 respectively. The difference indicates largely increasing sea level during the 1950s
419 and substantial interannual variability. These values are also relatively large compared
420 with the global mean value of 1.8 mm/yr derived from the records of 25 tide-gauge
421 stations around the world for the same period. Similar to the recent 15-year trend, this
422 relatively high value could be due to primarily regional influences. Note that the

423 recent increasing rate of SLR (1993~2003) is also much higher than (more than
424 double) the mean rate of the last 50 years. The ratio is consistent with the other global
425 estimates (IPCC, 2007), except that the rates we have observed are higher. In the next
426 section, we will further discuss the possible causes of the regional SLR around
427 Taiwan.

428

429 **4. Possible mechanisms for the long term trends**

430

431 **4.1 Upper ocean warming effect**

432

433 The results presented in Section 3 contain a large range of rates of relative sea level
434 change and indicate that the recent variations in the SLR are highly correlated with
435 the local OHC. In particular, the rates of increase have been relatively large over the
436 last 50 years and are evident from all records. Here, we further examine the historical
437 ocean thermal conditions (Ishii et al., 2006) in the upper ocean of the study area.

438

439 Antonov et al. (2005) and Ishii et al. (2006) estimated an approximate value of $1.2 \pm$
440 0.5 mm/yr for the global SLR (1993~2003) that is due to thermal expansion in the
441 upper 700 m. This is also subject to significant regional redistributions of heat and
442 spatially inhomogeneous patterns. Thus, more SLR may result from eustatic effects at
443 high latitudes while ocean warming may dominate at lower latitudes. Ishii et al. (2006)
444 showed that the thermosteric component is dominant in the sea level change around
445 Japan. They also found that tide-gauge agreement is usually better in areas where the
446 thermosteric effects are regarded as a dominant contributor to steric SLR. Figure 8 (a)
447 shows a LOESS analysis of the Ishii subsurface temperature anomaly data since 1946
448 at different depths (Ishii et al., 2006). The 0–300 m depth averaged temperature

449 anomaly is also shown as blue solid lines (without smoothing). We divided the $1^\circ \times 1^\circ$
450 resolution temperature data into three different regions: the SCS, WP and ECS. These
451 represent the regional seas to the south, east, and north of Taiwan. Similarly to the
452 other regions in the North Pacific, there is a consistent warming signal in Figure 8 (a).
453 The corresponding steric sea level variation for each region is also presented in Figure
454 8 (b), which shows clear thermal influences. Analysis of individual regions shows that
455 the upper layer temperature has increased by more than 1°C over the last 60 years.
456 The Pacific has been warming since the 1950s and two major peaks, in the 1950s and
457 the late 1990s, are observed. A minor warming peak in the late 1970s has also been
458 observed in WP and ECS, similar to those shown by the observed tide-gauge data near
459 Taiwan (e.g., there is positive but decreasing forward differences around the late
460 1950s and large positive forward differences around the 1970s and 1990s in Figure 5).
461 Most of the tide-gauge data correlates well with the steric height variation in the
462 nearby regions. For example, the correlation between the observed sea level variation
463 at station NH and the estimated steric height variation for ECS in Figure 8(b) can be
464 as high as 0.92. The lowest correlation is observed in station NS (0.48). Note that the
465 high sea levels usually correspond to high temperature anomalies at 100–300 m
466 depths (100 m depth shown as dashed lines and 200 m depth shown as dots), which
467 are particularly clear for the observed warming during the 1950s while the surface
468 temperature is cool. This suggests that, consistent with the nearby regions (e.g., Kang
469 et al., 2005), thermal expansion could be a major contributor to the observed SLR
470 around Taiwan, at least during the last 50~60 years.

471

472 Comparing the regional warming with the global ocean, Antonov et al. (2005) and
473 Ishii et al. (2006) estimated an average thermosteric trend of 0.33 mm/yr and 0.36
474 mm/yr, respectively, during the period 1955~2003. The rate of thermosteric SLR

475 varies significantly with time. Both the Levitus and Ishii data sets show that a
476 significant rise occurred from the late 1960s to the late 1970s with a small decrease
477 afterwards. Another large rise began in the 1990s but decreased after 2003. These
478 patterns indicate larger accelerations in the SLR during the 1950s, late 1970s, and late
479 1990s. Interestingly, they are quite consistent with the regional SLR trends shown in
480 Table 2 and Figures 5 and 8.

481

482 This evidence suggests that SLR in the regional seas around Taiwan tends to be
483 dominated by decadal signals in the regional OHC while the eustatic influence is
484 limited. This pattern may be associated with sea level variations in the entire Pacific
485 basin. Since the Pacific is strongly influenced by interannual variability associated
486 with ENSO (an ocean–atmosphere coupled mode in the climate system), the
487 ENSO-related ocean variability may account for the largest fraction of variance in
488 spatial patterns of thermosteric sea level which has caused the largest increases in
489 SLR in the last few decades (IPCC, 2007; Sun and Yu, 2009). Similarly, the observed
490 SLR trends (or thermosteric sea levels) could be partially associated with the Pacific
491 Decadal Oscillation (PDO) which may be related to the basin-wide regime shift that
492 occurred in 1976~1977. In either case, thermosteric effects most likely explain the
493 decadal variations we have observed in the regional tide-gauge data.

494

495 **4.2 Other possible factors**

496

497 **Other possible influences on sea level variations include changes in water masses as a**
498 **result of water exchange with other surface reservoirs, such as river inflow,**
499 **atmosphere, continental water, glaciers, and ice sheets (Church et al., 2004; IPCC,**
500 **2007). However, the eustatic contributions from the continents and melting sea ice**

501 (Antonov et al., 2002; Munk, 2003) may be locally significant on the decadal scales.
502 In the area of interest, one possible mass source is river discharge, which could only
503 cause small local steric increases in the sea level. Another possible water mass input
504 results from the atmosphere. This has not been well defined and quantified, and is a
505 topic that requires further study. Furthermore, the water impounded by the artificial
506 reservoirs could cause the negative feedback for SLR (Chao et al., 2008). These
507 overall water mass changes are difficult to estimate based on available observations.
508 We find there is little evidence for eustatic contributions to the observed SLR in the
509 regional seas around Taiwan.

510

511 Ocean circulation changes may also cause sea level variations. To the best of our
512 knowledge, the long-term regional ocean circulation has not changed significantly in
513 terms of the overall transport. Finally, tectonic movements or local subsidence (e.g.,
514 due to groundwater withdrawal and terrestrial storage) could introduce a large amount
515 of uncertainty. Some stations may be subsiding, thus giving even higher apparent SLR
516 rates. Other relevant results show that local subsidence is occurring along many
517 coastal regions in Asia. This could be due to the draining of underground aquifers in
518 coastal regions to supply fresh water. However, the observations acquired during
519 different periods show that long-term relative sea level variations should not be
520 significantly affected by local effects. These factors may only contribute to the
521 observed inhomogeneous patterns between the stations but do not affect the similarity
522 of the long-term trends dominated by regional sea level evolution.

523

524 **5. Summary**

525

526 We present sea level information or trends and variability over a 50-year period for

527 the regional seas around Taiwan. Similar trends and patterns are detected at most
528 stations. For the period 1993~2003, the available tide-gauge records show an average
529 rate of SLR of about 5.7 mm/yr, which is more than twice that observed during
530 1961~2003 (2.4 mm/yr). This implies that there have been higher accelerations in
531 SLR in recent decades. The rise rate is quite consistent with previous estimates from
532 nearby areas in the western Pacific and is generally higher than the global mean.
533 Larger spatial and temporal variations are also found in the tide-gauge data.

534

535 Satellite altimetry is also used to verify the regional sea level variations over the past
536 15 years. For the period 1993~2003, the altimetry-derived SLR is 5.3 mm/yr. There is
537 good agreement between the altimetry and the tide-gauge data. Further comparisons
538 with regional OHC suggest that thermal expansion and heat advection in the upper
539 layer make a significant contribution to long-term sea level variations in this area (the
540 correlation is higher than 0.9). Specifically, thermosteric sea level variations appear to
541 dominate the observed SLR around Taiwan. The interannual and decadal oscillations
542 in sea level could result from coupled ocean–atmospheric climate perturbations such
543 as ENSO and/or the PDO in the North Pacific.

544

545 Based on the tide-gauge data, the long-term regional patterns in sea level show clear
546 decadal scale variations. Since the altimetry records are relatively short, the long-term
547 trend of SLR can only be estimated from the tide-gauge records. Our results suggest
548 that the time series signal from the altimetry is only part of a longer-term and
549 larger-scale signal. This implies that extrapolating SLR to future scenarios using only
550 satellite altimetry (after 1993) requires caution. Further study of the ocean heat budget
551 could provide additional information on the cause of the decadal oscillation in the
552 OHC, which is presently not well understood. Further studies based on general ocean

553 circulation models are required.

554 **Reference:**

555

556 Antonov, J. I., S. Levitus, and T. P. Boyer (2002), Steric sea level variations during
557 1957-1994: Importance of salinity, *Journal of Geophysical Research-Oceans*, 107,
558 doi: 10.1029/2001jc000964.

559 Breaker, L. C. (2007), A closer look at regime shifts based on coastal observations
560 along the eastern boundary of the North Pacific, *Continental Shelf Research*, 27,
561 2250-2277.

562 Cabanes, C., A. Cazenave, and C. Le Provost (2001), Sea level rise during past 40
563 years determined from satellite and in situ observations, *Science*, 294, 840-842.

564 Cazenave, A., and R. S. Nerem (2004), Present-day sea level change: Observations
565 and causes, *Reviews of Geophysics*, 42, RG3001, doi:10.1029/2003rg000139.

566 Chang, E. T.Y. C., C. Chiang, B.F. Chao, and C.W. Hwang (2009), Vertical plate
567 motion in the vicinity of active plate convergence (*submitted to Geophysical*
568 *Research Letters*).

569 Chao, B.F., Y. H. Wu and Y. S. Li (2008), Impact of artificial reservoir water
570 impoundment on global sea level, *Science*, 320, 212-214.

571 Chelton, D. B. and D. B. Enfield (1986), Ocean signals in tide gauge records. *Journal*
572 *of Geophysical Research*, 91, 9081-9098.

573 Chen, X. Q. (1991), Sea-level changes since the early 1920s from the long records of
574 2 tidal gauges in Shanghai, China, *Journal of Coastal Research*, 7, 787-799.

575 Cheng, X. H., and Y. Q. Qi (2007), Trends of sea level variations in the South China
576 Sea from merged altimetry data, *Global and Planetary Change*, 57, 371-382.

577 Church, J. A., N. J. White, R. Coleman, K. Lambeck, and J. X. Mitrovica (2004),
578 Estimates of the regional distribution of sea level rise over the 1950-2000 period,
579 *Journal of Climate*, 17, 2609-2625.

580 Cleveland, W. S., and S. J. Devlin (1988), Locally weighted regression: An approach
581 to regression analysis by local fitting, *Journal of the American Statistical*
582 *Association*, 83, 596-610.

583 Cleveland, W. S. (1979), Robust locally weighted regression and smoothing
584 scatterplots, *Journal of the American Statistical Association*, 74, 829-836.

585 Douglas, B. C. (1997), Global sea rise: A redetermination, *Surveys in Geophysics*, 18,
586 279-292.

587 Emery, W. J. and R. E. Thomson (2004), Data analysis methods in Physical
588 Oceanography, Elsevier, Amsterdam. 638pp.

589 Hastie, T., and R. Tibshirani (1990), Exploring the nature of covariate effects in the
590 proportional hazards model, *Biometrics*, 46, 1005-1016.

591 Ho, C. S. (1986), A synthesis of the geologic evolution of Taiwan, *Tectonophysics*,
592 125, 1-16, 1986.

593 IPCC (2007), Climate Chang 2007: The physical science basis. Summary for policy
594 makers. Contribution of working group I to the fourth assessment report. The
595 Intergovernmental Panel on Climate Change, <http://www.ipcc.ch/SPM2feb07.pdf>

596 Ishii, M., M. Kimoto, K. Sakamoto, and S. I. Iwasaki (2006), Steric sea level changes
597 estimated from historical ocean subsurface temperature and salinity analyses,
598 *Journal of Oceanography*, 62, 155-170.

599 Kang, S. K., J. Y. Cherniawsky, M. G. G. Foreman, H. S. Min, C. H. Kim, and H. W.
600 Kang (2005), Patterns of recent sea level rise in the East/Japan Sea from satellite
601 altimetry and in situ data, *Journal of Geophysical Research-Oceans*, 110, doi:
602 10.1029/2004jc002565.

603 Levitus, S., J. I. Antonov, T. P. Boyer, and C. Stephens (2000), Warming of the world
604 ocean, *Science*, 287, 2225-2229.

605 Levitus, S., J. Antonov, and T. Boyer (2005), Warming of the world ocean,

606 1955-2003, *Geophysical Research Letters*, 32, doi: 10.1029/2004gl021592.

607 Li, L., J. D. Xu, and R. S. Cai (2002), Trends of sea level rise in the South China Sea
608 during the 1990s: An altimetry result, *Chinese Science Bulletin*, 47, 582-585.

609 Lisitzin, E. 1974. *Sea Level Changes*. Elsevier Oceanography Series (8), Elsevier,
610 Amsterdam.

611 Metzger, E. J. and H. E. Hurlbert (2001), The importance of high horizontal resolution
612 and accurate coastline geometry in modeling South China Sea inflow, *Geophys.*
613 *Res.Lett.*, 101, 12331-12352.

614 Miller, L., and B. C. Douglas (2004), Mass and volume contributions to
615 twentieth-century global sea level rise, *Nature*, 428, 406-409.

616 Munk, W. (2003), Ocean freshening, sea level rising, *Science*, 300, 2041-2043.

617 Ose, T., Y. K. Song, and A. Kitoh (1997), Sea surface temperature in the South China
618 Sea - an index for the Asian monsoon and ENSO system, *Journal of the*
619 *Meteorological Society of Japan*, 75, 1091-1107.

620 Palmer, M. D., K. Haines, S. F. B. Tett, and T. J. Ansell (2007), Isolating the signal of
621 ocean global warming, *Geophysical Research Letters*, 34, L23610,
622 doi:10.1029/2007gl031712.

623 Sun, F., J.-Y. Yu (2009), A 10-15 year Modulation cycle of ENSO intensity, *Journal*
624 *of Climate*, 22, 1718-1735.

625 Schrama, E., R. Scharroo, and M. Naeije (2000), Radar Altimeter Database System
626 (RADS): Towards a generic multi-satellite altimeter database system, final report,
627 88, *SRON/BCRS publ., USP-2 report 00-11*.

628 Tushingham, A. M., and W. R. Peltier (1991), Ice-3G- A new global-model of late
629 pleistocene deglaciation based upon geophysical predictions of postglacial relative
630 sea-level change, *Journal of Geophysical Research-Solid Earth and Planets*, 96,
631 4497-4523.

- 632 Wang, Y. (1998), Sea-Level Changes, Human impacts and coastal responses in China,
633 *Journal of Coastal Research*, 14, 31-36.
- 634 Woodworth, P. L., and R. Player (2003), The permanent service for mean sea level:
635 An update to the 21st century, *Journal of Coastal Research*, 19, 287-295.
- 636 Xie, S. P., Q. Xie, D. X. Wang, and W. T. Liu (2003), Summer upwelling in the South
637 China Sea and its role in regional climate variations, *Journal of Geophysical*
638 *Research-Oceans*, 108, doi: 10.1029/2003cj001867.

Table 1: Tide-gauge stations in the regional seas around Taiwan (used in this study). The official code numbers are directly obtained from the CWB and PSMSL records.

Station/official code number			Location	Time(year,month)	Source	Final Series
Hong Kong(HK)	QB	611010	22.3°N, 114.2°E	198601~200612	PSMSL	195004~200612
	NP	611011		192904~198512		
	TP	611014		196301~200612		
Kanmen (KM)	610016		28.1°N, 121.3°E	195901~200712	PSMSL	195901~200712
Kaohsiung (KS)	148		22.6°N, 120.3°E	198701~200807	CWB	194705~200712
	1481			199707~199806		
	1482			194705~198612		
	1486			200403~200808		
	612012			197301~198912	PSMSL	-
Keelung (KL)	1212		25.2°N, 121.7°E	194605~199012	CWB	194801~200612
	151			199503~200012		
	1511			199101~199503		
	1513			200401~200712		
	1516			200711~200808		
	612002			195601~199512	PSMSL	-
NAHA (NH)	646024		26.2°N, 127.7°E	196608-200712	PSMSL	196608~200712
NASE (NS)	I	646001	28.4°N, 129.5°E	195704~196112	PSMSL	195701~200712
	II	646002		196201~198012		
	III	646003		198101~200712		
Penghu (PH)	1351		23.5°N, 119.5°E	195503~200612	CWB	195503~200612
Xiamen (XM)	610016		24.5°N, 118.1°E	195501~200412	PSMSL	195501~200412

Table 2: Mean sea level rise (mm/yr) from the tide gauges and altimetry (estimated by LOESS analysis)

	1993~2003	1961~2003	1955~2003	Entire periods
Hong Kong (HK)	4.0	2.1	0.2	0.6 (1951~2006)
Kanmen (KM)	2.0	1.7	-	1.4 (1960~2007)
Kaohsiung (KS)	7.3	4.9	3.4	1.9 (1949~2006)
Keelung (KL)	-0.3	0.8	0.5	0.8 (1948~2006)
NAHA (NH)	3.5	2.5	-	3.4 (1968~2007)
NASE (NS)	4.3	0.4	-	-0.1 (1959~2007)
Penghu (PH)	17.1	4.3	11.0	10.5 (1956~2006)
Xiamen (XM)	7.8	2.7	2.3	2.3 (1955~2003)
Mean (tide gauges)	5.7	2.4	3.5	
Mean (altimetry)	5.3			5.0 (1993~2007)
Global (IPCC, 2007)	3.1	1.8		

Figure captions:

Figure 1: The regional seas around Taiwan and the tide-gauge stations used in this study. Taiwan is surrounded by South China Sea (SCS), Philippine Sea (PS), East China Sea (ECS) and Taiwan Strait. Taiwan Strait is a 200-km-wide shallow passage between Taiwan and China. The tectonic plates are also shown. Abbreviated terms are as follows: JP: Japan, here is the Kyushu island; PH: Philippine, here is the northern Luzon; TW: Taiwan. A major fault line constitutes a convergent boundary east Taiwan (yellow lines). The information about tide gauge stations is detailed in Table 1.

Figure 2: The altimetry tracks used in this study represent in black dash-lines; their track numbers are indicated. The adopted segments for determined SRL are zoned by yellow rectangles, which are selected around Taiwan with five regions (A-E).

Figure 3: Monthly observations of relative sea levels and their trends at (a) Hong Kong (HK) and Kaohsiung (KS); and (b) Xiamen (XM) and Penghu (PH). Two nearby observations (HK and TP, see Table 1) are shown in Hong Kong according to the records in PSMSL. HK combines the original data from two continuous stations (QB and NP, see Table 1). The straight lines are the linear trends for the whole observation period based on robust linear regression while the red solid curves are the non-linear variations estimated by the LOESS analysis (see texts). Eighteen months moving mean filters (shown as dash lines) are also applied to the scattered observation (shown as dots) in order to remove the annual or other high frequency signal.

Figure 4: Same as Figure 3 but for different tide-gauge stations. (a) Keelung (KL) and Kanmen (KM); and (b) NASE (NS) and NAHA (NH) in Japan.

Figure 5: Comparison of the yearly forward first differences of the LOESS analysis for all stations. The curves show the change in sea levels each year (mm/yr). The average of all slopes during a particular period represents the long-term mean slope (i.e. linear trend) for that period.

Figure 6: The altimetry derived rates of sea level variation during 1993-2007 in the regional seas around Taiwan at different locations (See Figure 2). The straight dash-dotted lines are the linear trends for the whole observation period based on robust linear regression while the solid curves are the non-linear variations estimated by the LOESS analysis. Eighteen months moving mean filters (shown as dash lines) are also applied. The variation of temperature anomaly in the Pacific is also shown here (top panel) for comparison (black solid line, Palmer et al., 2007).

Figure 7: The comparison between the altimetry-derived (location E) and tidal gauge (KS) observed

sea level variations. Both eighteen months moving-averaged (MV) time-series and non-linear LOESS analysis results are shown. The time-series, depth integrated (down to 300 m) temperature anomaly in the northeast SCS is also shown here as a thick solid line (Ishii et al., 2006).

Figure 8: the LOESS analysis of the ocean subsurface temperature and steric height anomaly since 1946 (Ishii et al., 2006). (a) Top three panels: SCS, WP and ECS, respectively. The temperature anomaly at 0 (solid lines), 50 (dashed dot lines), 100 (dashed lines) and 200 (dots) m depth. The 0-300 m depth averaged temperature anomaly is also shown as the blue solid lines (without LOESS smoothing). (b) Bottom panel: The derived steric height for three chosen regions.

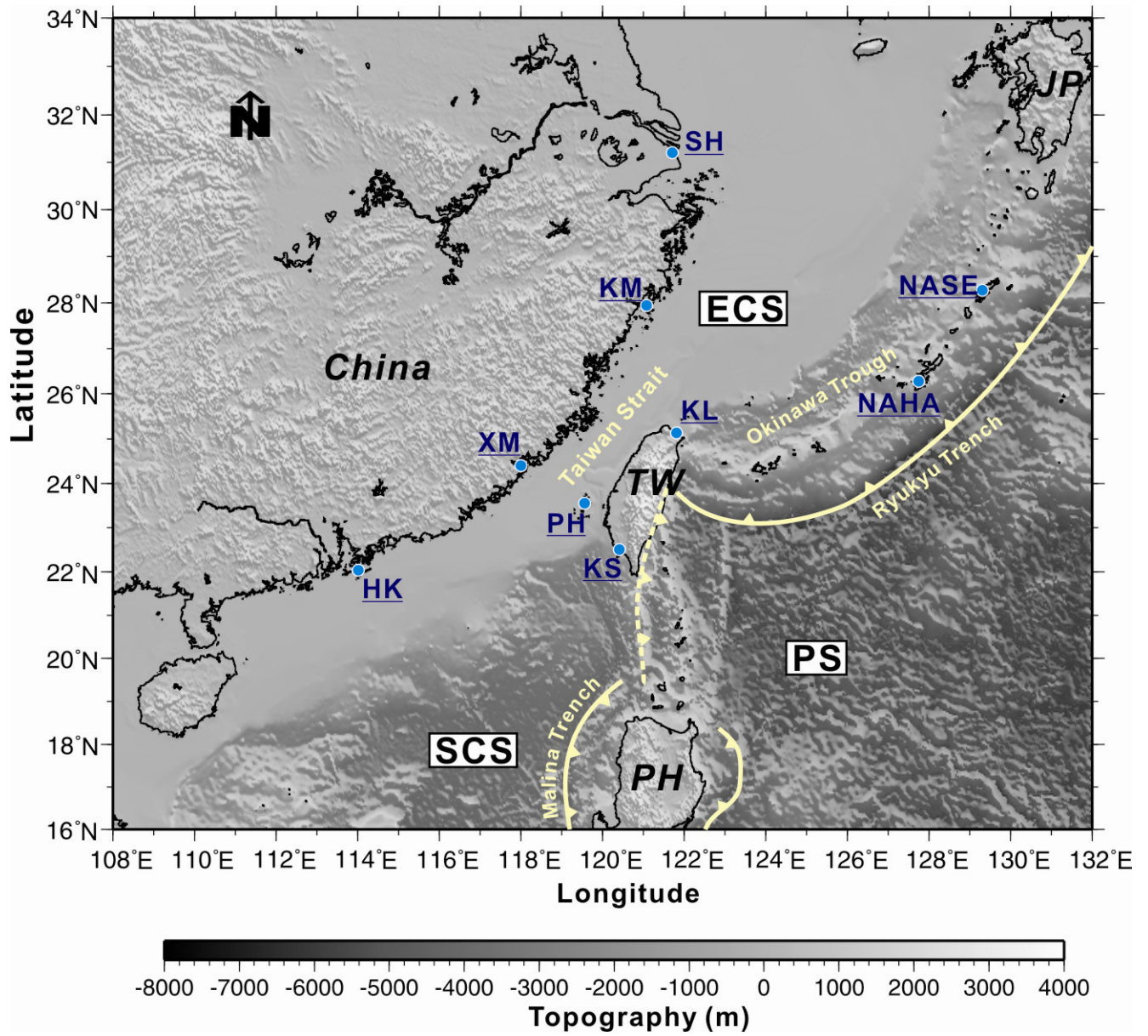


Figure 1

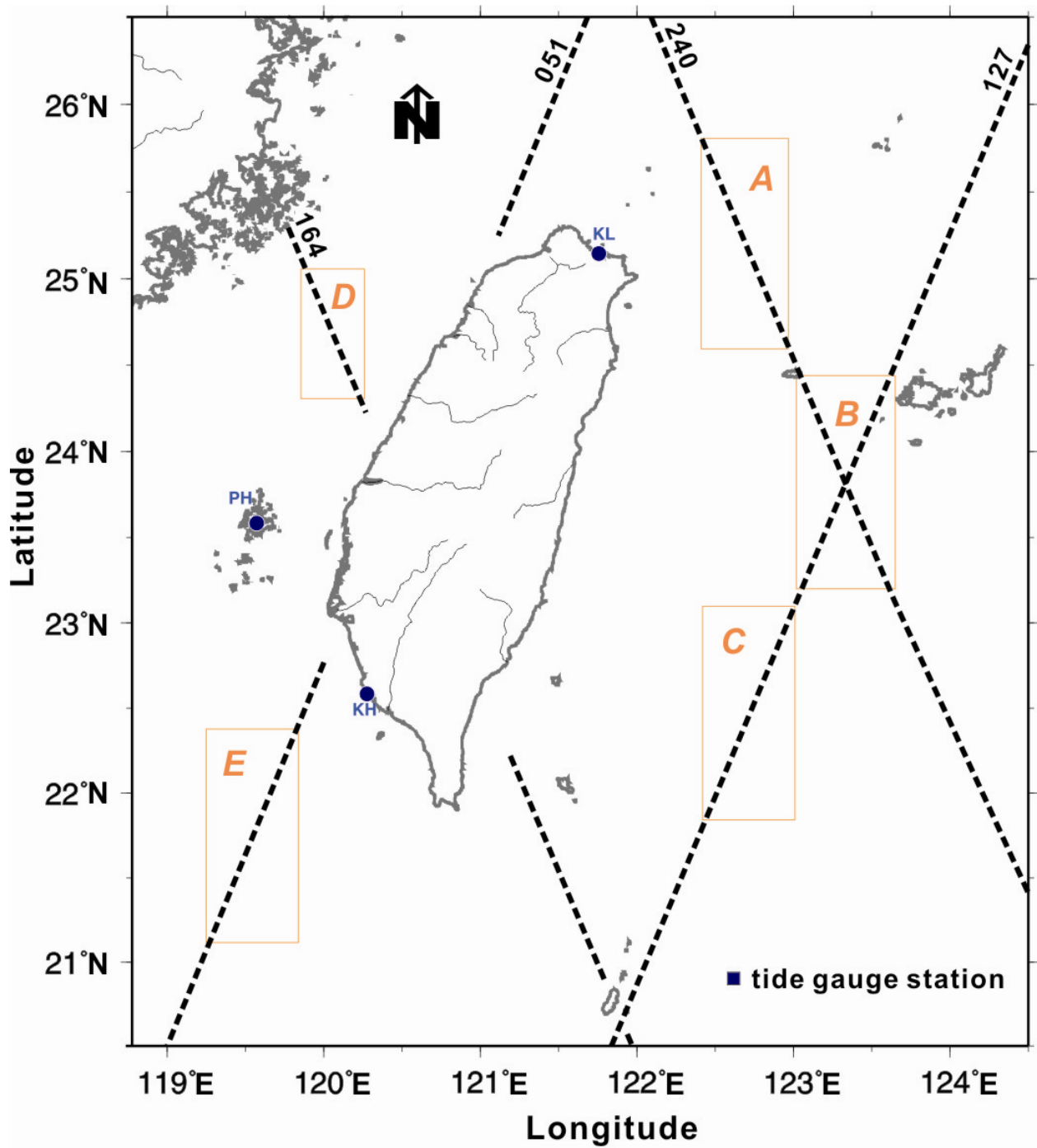
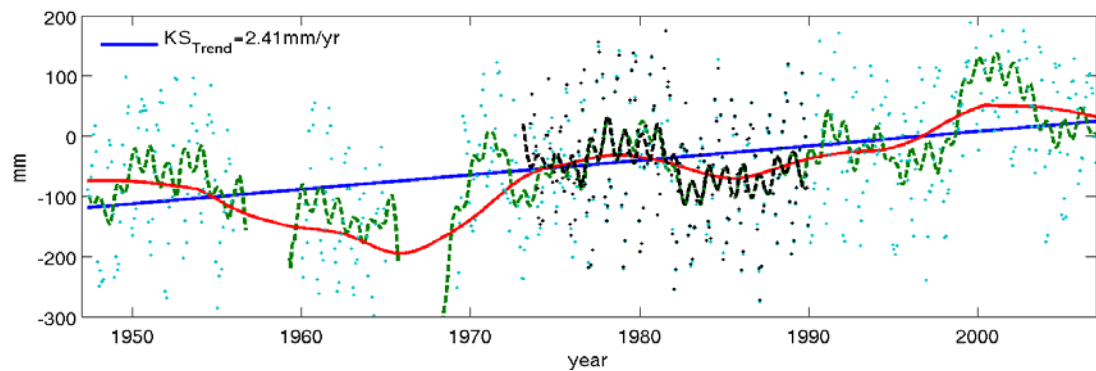
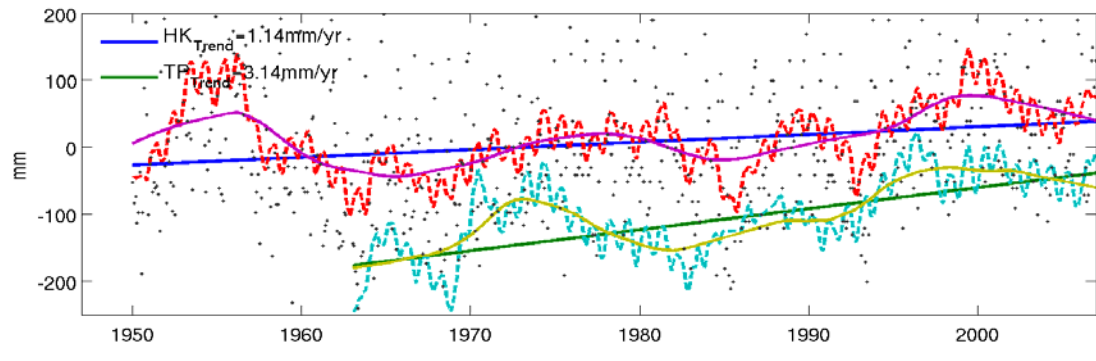
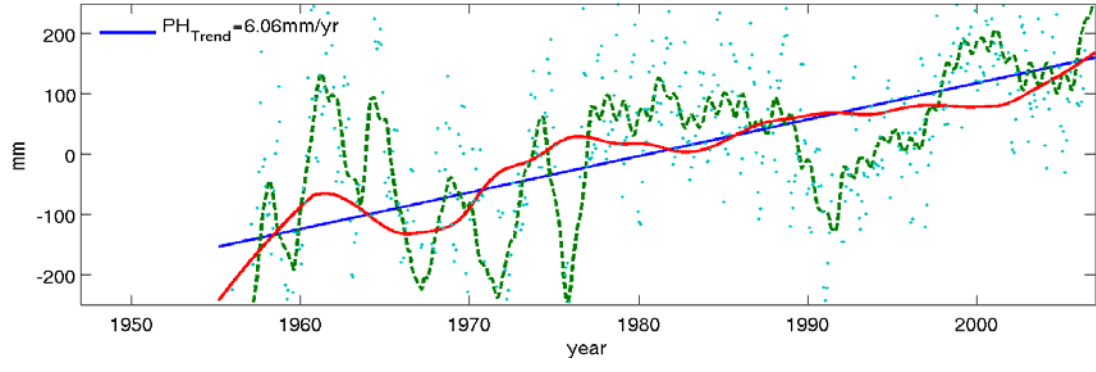
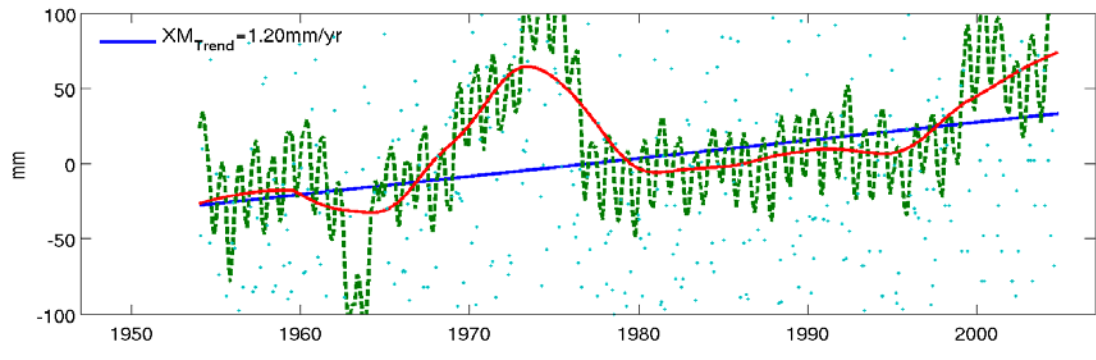


Figure 2

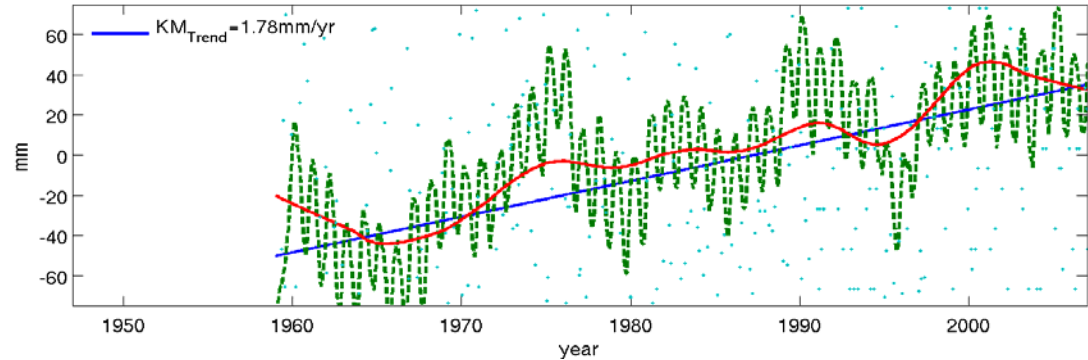
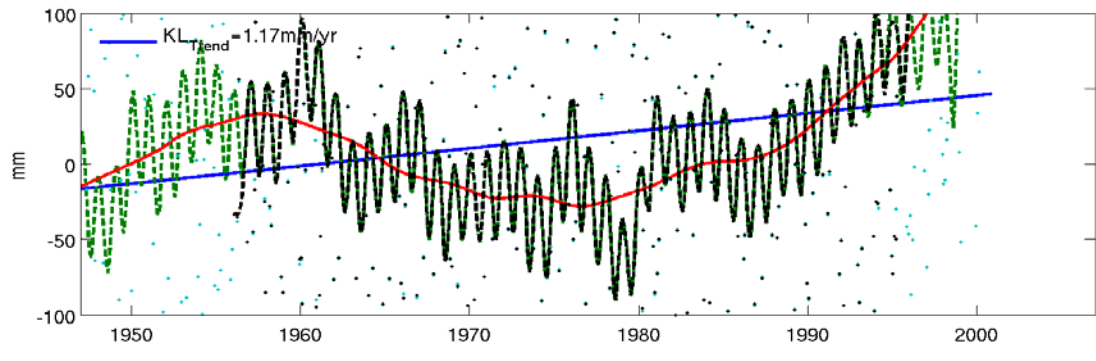


(a)

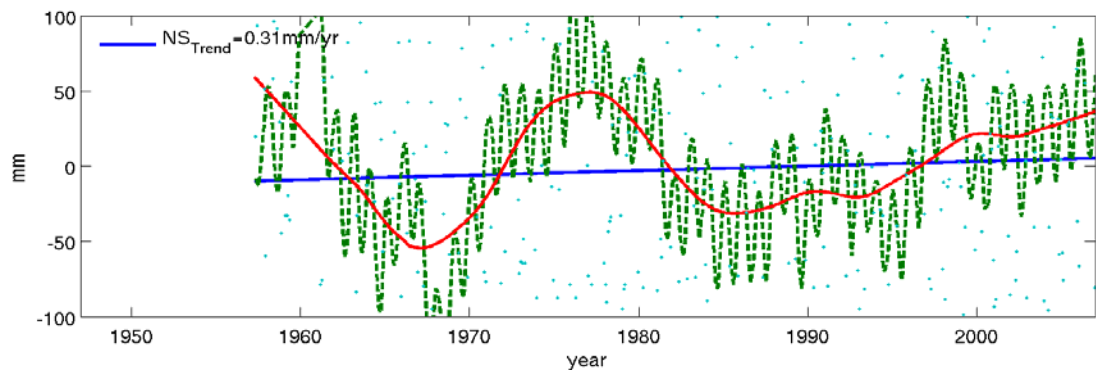
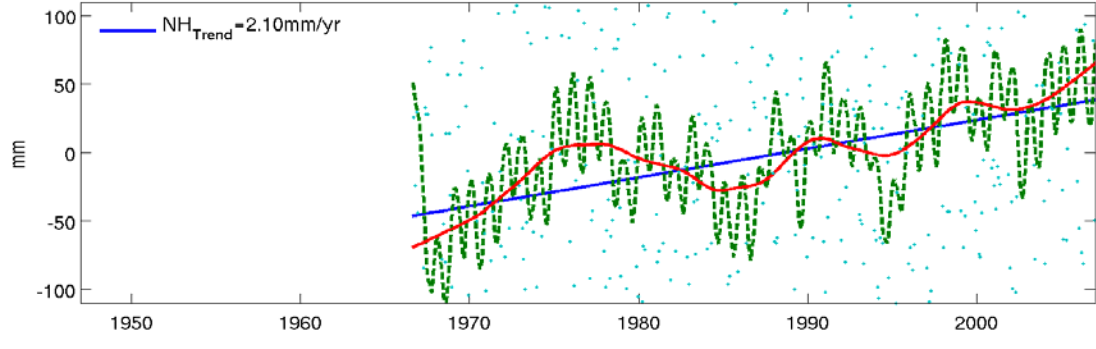


(b)

Figure 3

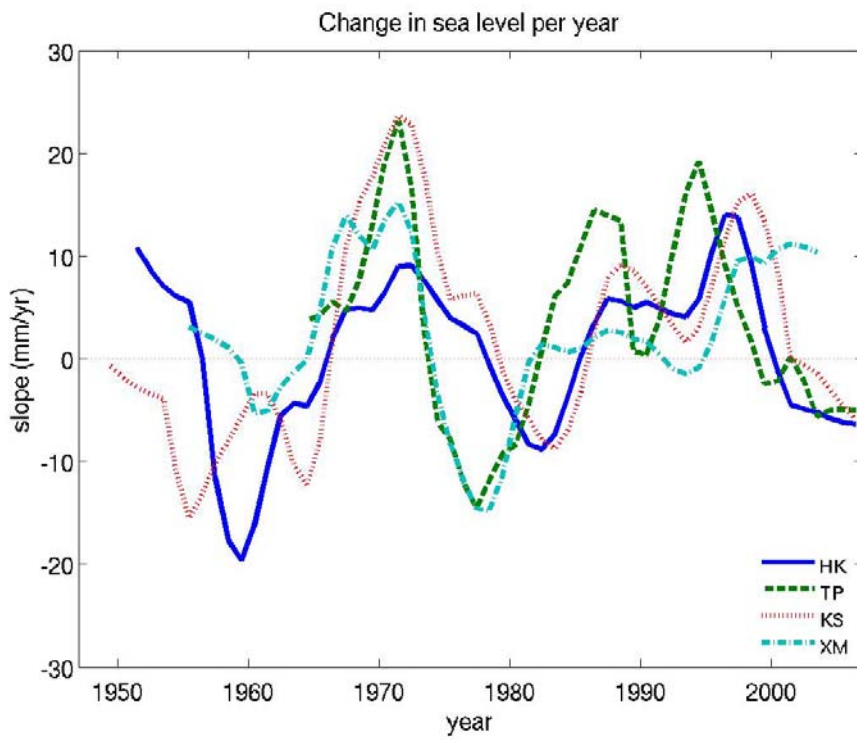


(a)

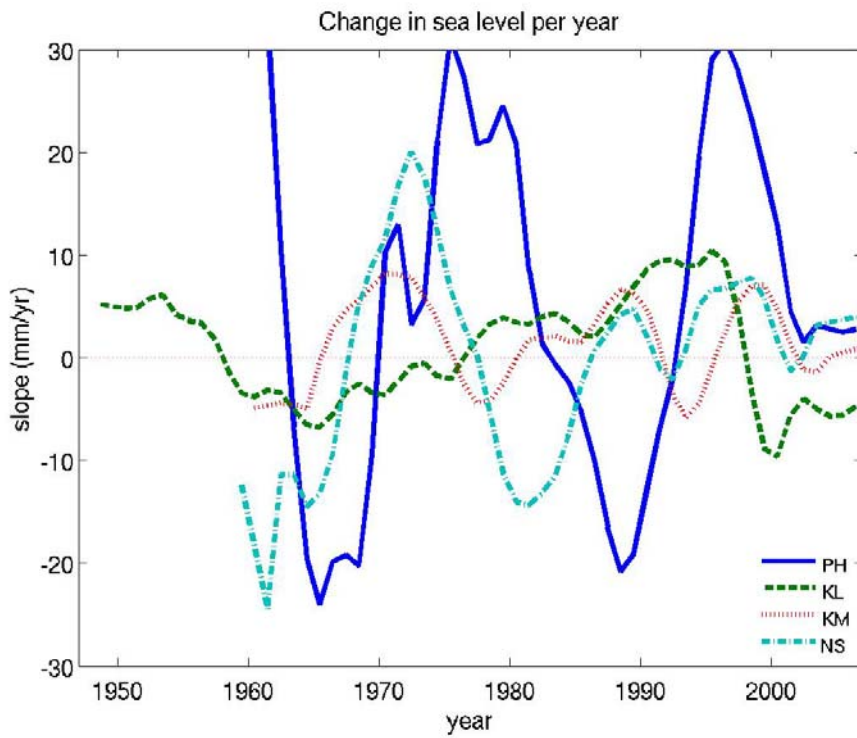


(b)

Figure 4



(a)



(b)

Figure 5

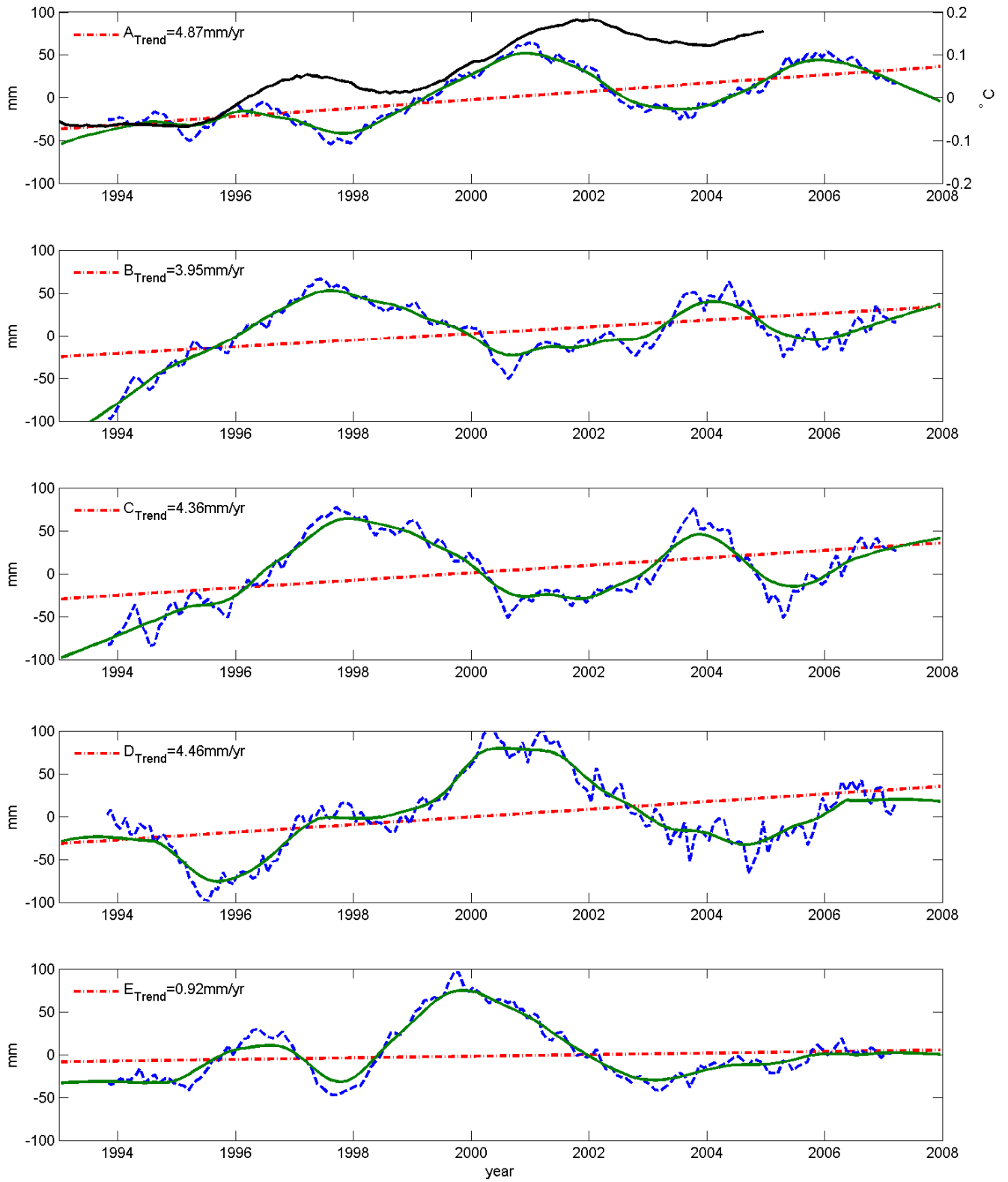


Figure 6

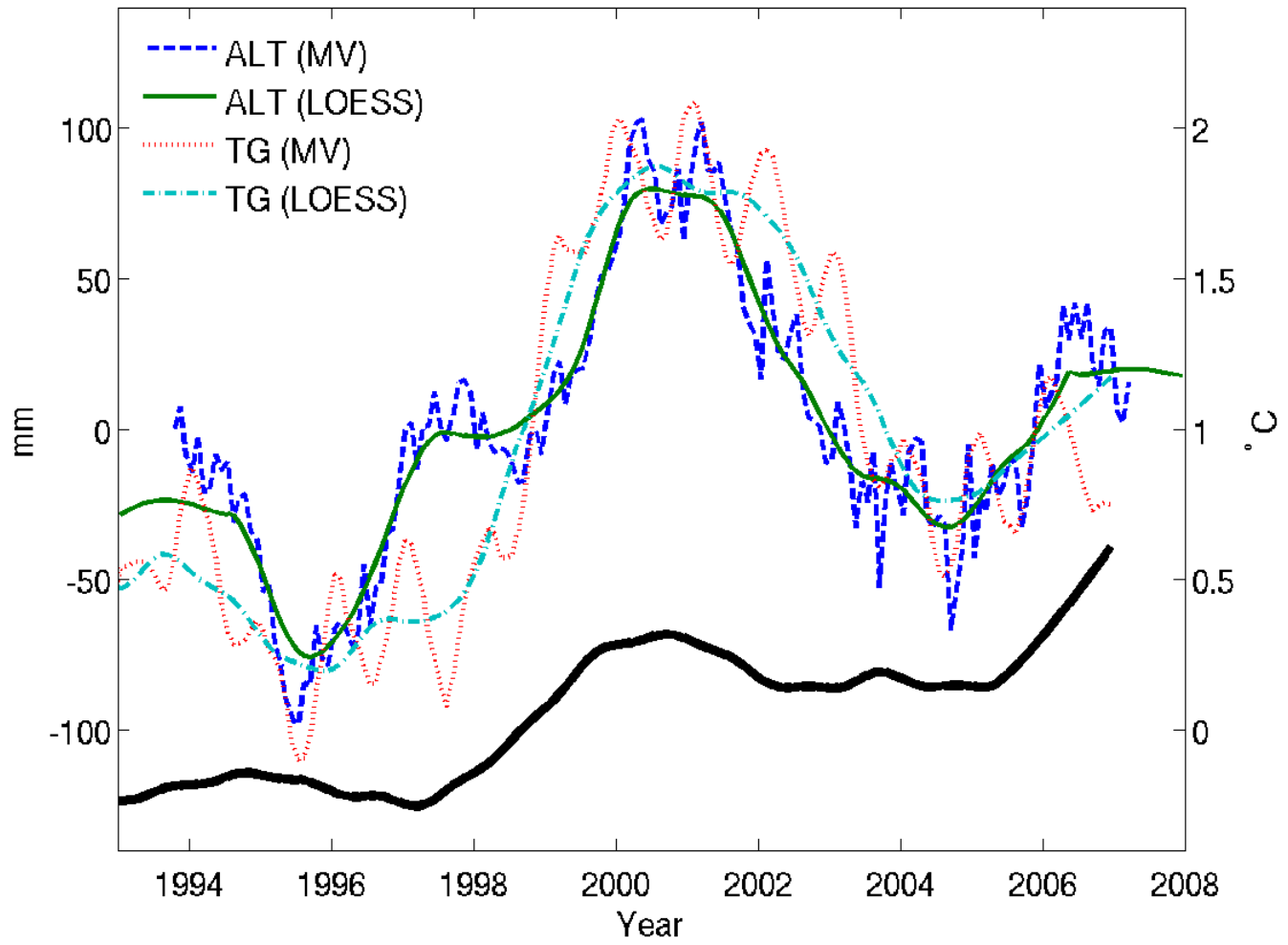


Figure 7

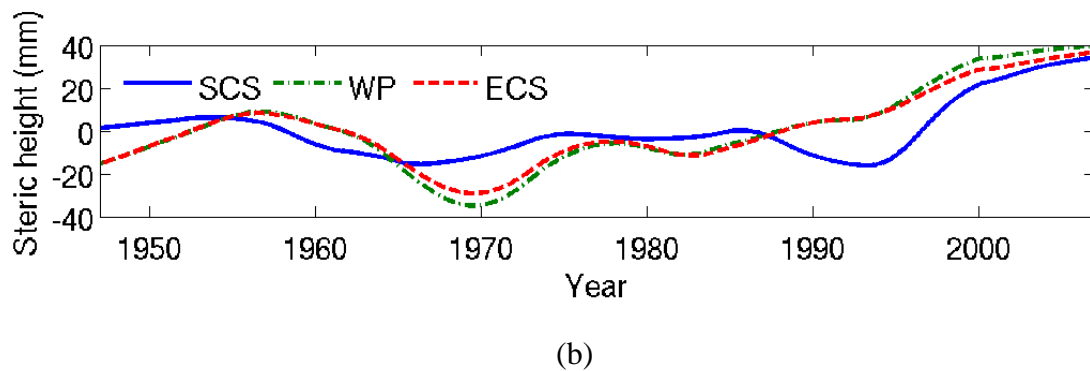
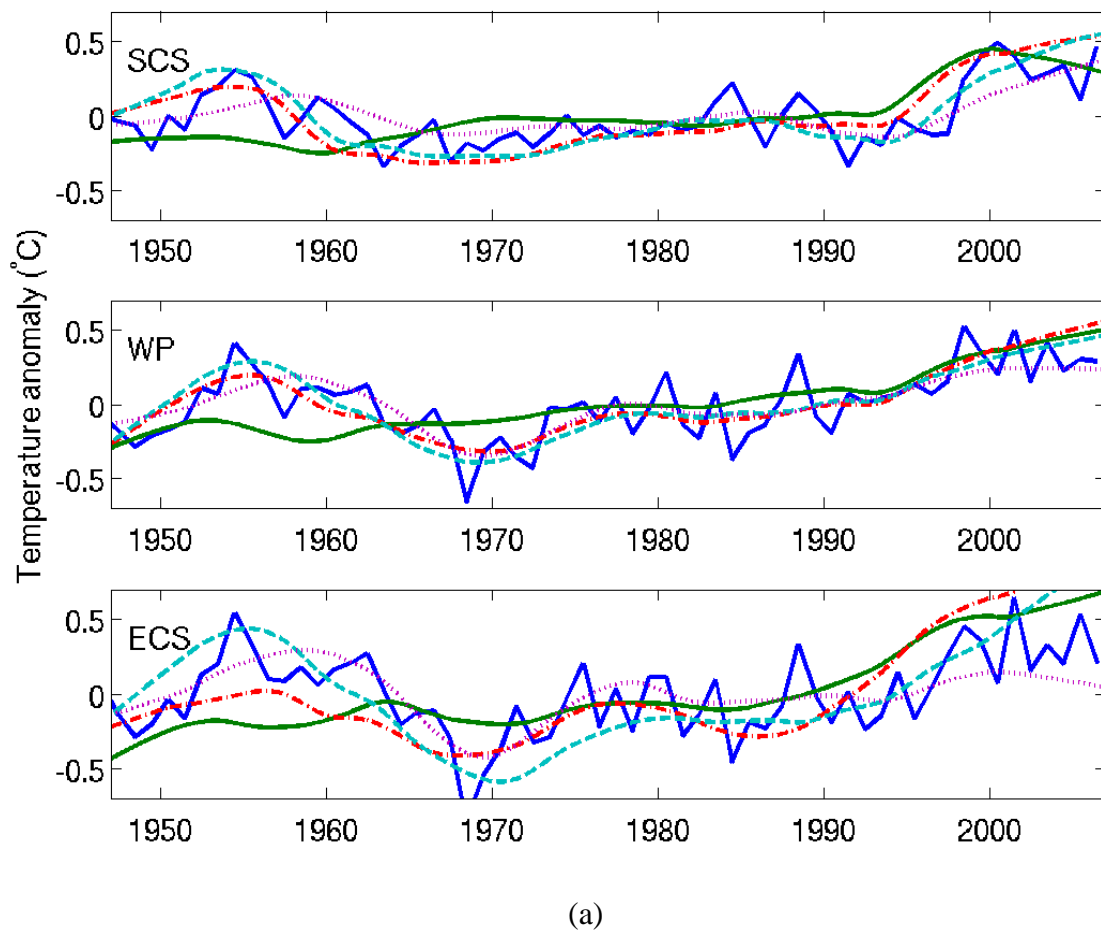


Figure 8

Table 2: IPCC (2007)

Steric sea level change with errors (mm yr ⁻¹)	Period	Depth Range (m)	Data Source
0.40±0.09	1955~1998	0-3000	Levitus et al. (2005b)
0.33±0.07	1955~2003	0-700	Levitus et al. (2005b)
0.36±0.06	1955~2003	0-700	Ishii et al. (2006)
1.2±0.5	1993~2003	0-700	Levitus et al. (2005b)
1.2±0.5	1993~2003	0-700	Ishii et al. (2006)
1.6±0.5	1993~2003	0-750	Willis et al. (2004)
1.8±0.4	1993~2003	0-700	Guinehut et al. (2004)

Table 3: Sea Level Rise (mm/yr)

Source	1961-2003	1993-2003
Thermal Expansion	0.42±0.12	1.6±0.5
Glaciers and Ice Caps	0.50±0.18	0.77±0.22
Greenland Ice Sheet	0.05±0.12	0.21±0.07
Antarctic Ice Sheet	0.14±0.41	0.21±0.35
Sum	1.1±0.5	2.8±0.7
Observed	1.8±0.5	
		3.1±0.7
Difference(Observed-Sum)	0.7±0.7	0.3±1.0